# Joint In-Phase and Quadrature Non-Orthogonal Multiple Access for Multi-User VLC

Yuru Tang , *Graduate Student Member, IEEE*, Chen Chen , *Senior Member, IEEE*, Cuiwei He , *Member, IEEE*, Bohua Deng , Min Liu , Xinke Tang , H. Y. Fu , *Senior Member, IEEE*, and Harald Haas , *Fellow, IEEE* 

Abstract-In this paper, we propose and demonstrate a new non-orthogonal multiple access (NOMA) scheme named joint inphase and quadrature NOMA (JIQ-NOMA) for a multi-user visible light communication (VLC) system. In contrast to the conventional NOMA scheme, JIQ-NOMA independently employs NOMA in both the in-phase (I) and quadrature (Q) domains, utilizing pulse amplitude modulation (PAM). Therefore, an additional degree of freedom for power allocation is introduced, enabling a more efficient solution to address the user unfairness issue in NOMA. Moreover, to optimize the system performance, we also introduce a two-dimensional (2D) power allocation method, which includes I domain/Q domain (I/Q) power allocation to ensure fairness among users within each user pair and joint I domain and Q domain (JIQ) power allocation to guarantee fairness among different user pairs. Simulation and experimental evaluations are both conducted under various channel conditions to validate the benefits of the proposed JIQ-NOMA scheme over conventional orthogonal multiple access (OMA) and NOMA schemes. Experimental results show that, in a four-user VLC system, when applying the proposed JIQ-NOMA scheme compared to the conventional NOMA scheme, the required peak-to-peak voltage (Vpp) used to drive the light-emitting diode (LED) transmitter can be reduced by 21.5%, and the transmission distance can be extended by 16.7% at a target bit error rate (BER) of  $3.8 imes 10^{-3}$ .

Index Terms—Non-orthogonal multiple access (NOMA), user fairness, visible light communication (VLC).

Manuscript received 20 December 2023; revised 4 June 2024; accepted 12 June 2024. Date of publication 14 June 2024; date of current version 16 October 2024. This work was supported in part by the National Natural Science Founation of China under Grant 62271091 and Grant 61901065, and in part by the Natural Science Foundation of Chongqing under Grant cstc2021jcyjmsxmX0480. (Corresponding authors: Chen Chen; H. Y. Fu.)

Yuru Tang and H. Y. Fu are with the Tsinghua Shenzhen International Graduate School, Tsinghua University, Shenzhen 518055, China, and also with the Peng Cheng Laboratory (PCL), Shenzhen 518055, China (e-mail: tyr23@mails.tsinghua.edu.cn; hyfu@sz.tsinghua.edu.cn).

Chen Chen and Min Liu are with the School of Microelectronics and Communication Engineering, Chongqing University, Chongqing 400044, China (e-mail: c.chen@cqu.edu.cn; liumin@cqu.edu.cn).

Cuiwei He is with the School of Information Science Japan Advanced Institute of Science and Technology, Nomi 923-1211, Japan (e-mail: cuiweihe@jaist.ac.jp).

Bohua Deng is with the Tsinghua Shenzhen International Graduate School, Tsinghua University, Shenzhen 518055, China (e-mail: hyfu@sz.tsinghua.edu.cn).

Xinke Tang is with the Peng Cheng Laboratory (PCL), Shenzhen 518055, China (e-mail: tangxk@pcl.ac.cn).

Harald Haas is with the Technology Innovation Centre and the Department of Electronic and Electrical Engineering, University of Strathclyde, G1 1RD Glasgow, U.K. (e-mail: harald.haas@strath.ac.uk).

Color versions of one or more figures in this article are available at https://doi.org/10.1109/JLT.2024.3414834.

Digital Object Identifier 10.1109/JLT.2024.3414834

# I. INTRODUCTION

ITH the exponential growth in wireless data traffic, radio frequency (RF)-based wireless networks are becoming increasingly congested and are expected to reach saturation in the near future [1]. Optical wireless communication (OWC), viewed as a promising technology to augment RF communications, is widely considered for future 6G mobile networks [2], [3], [4], [5]. One form of OWC, known as visible light communication (VLC), utilizing light-emitting diodes (LEDs) for both indoor illumination and data transmission, has garnered significant interest in both academia and industry due to many of its advantages, including immunity to electromagnetic interference, low cost, high physical-layer security, and unregulated spectrum availability [6], [7], [8]. However, despite the broad optical spectrum of visible light, ranging from about 380 nm to 780 nm, the incoherent nature of the light emitted from LEDs means that only intensity modulation is suitable. Furthermore, the modulation bandwidth of commercial off-the-shelf optical components used in VLC is typically limited. For instance, the 3-dB bandwidth of typical white LEDs is only a few megahertz [9]. The limited modulation bandwidth in VLC poses challenges in designing suitable multiple access schemes that allow a single LED access point (AP) to simultaneously connect multiple high-speed users [10].

To date, various multiple access schemes have been proposed and applied in multi-user VLC systems, mainly categorized into two types: orthogonal multiple access (OMA) and nonorthogonal multiple access (NOMA). In OMA-based multi-user VLC systems, users are assigned orthogonal resources in the time/frequency/code domain [11], [12], [13], ensuring that information intended for different users can be decoded without interference. However, when OMA is used in LED-based VLC systems, the number of supported users is usually very constrained due to the limited orthogonal resources. To address this challenge, the concept of NOMA, originally proposed for RF systems, has been adapted into VLC systems [14], [15], [16], [17], [18]. In NOMA-based VLC systems, multiple users can be supported through the implementation of power-domain superposition coding (SPC) at the transmitter and successive interference cancellation (SIC) at the receiver. Although the use of NOMA introduces non-negligible multi-user interference compared to OMA systems, it is generally feasible to multiplex two users in the power domain when they share the same time and frequency resources, and their data can still be decoded

0733-8724 © 2024 IEEE. Personal use is permitted, but republication/redistribution requires IEEE permission. See https://www.ieee.org/publications/rights/index.html for more information.

successfully [19]. To support more than two users in VLC systems, a hybrid NOMA and orthogonal frequency-division multiple access (OFDMA) scheme has been considered by dividing all the users into multiple pairs [20], [21]. Specifically, considering the computational complexity and time delay to perform SIC, each user pair is assumed to contain only two users, which are multiplexed in the power domain via NOMA [3], [19]. Then, the multiplexing of various user pairs is achieved in the frequency domain via OFDMA.

Despite the many advantages of employing NOMA in VLC, a significant challenge is the issue of user fairness. This is because, in VLC, the channel gain of a user heavily depends on its location. Differences in location among users often result in performance imbalances when NOMA is used, thereby limiting overall transmission performance. In this paper, to enhance fairness among users with significantly different channel gains in practical multi-user VLC systems, we propose the joint inphase and quadrature NOMA (JIQ-NOMA) scheme. Compared with conventional NOMA, the proposed JIQ-NOMA scheme utilizes both the in-phase (I) domain and the quadrature (Q) domain to perform NOMA individually with pulse amplitude modulation (PAM). This approach, in contrast to conventional NOMA, provides an additional degree of freedom for power allocations to address the user fairness problem. Furthermore, a two-dimensional (2D) power allocation method is introduced in this paper to ensure fairness among users with different channel gains. Specifically, I domain/Q domain (I/Q) power allocation is performed to ensure fairness between two users within each user pair, while joint I domain and Q domain (JIQ) power allocation is performed to ensure fairness among different user pairs. Overall, the main contributions of this work are summarized as follows:

- A new NOMA scheme named JIQ-NOMA is proposed, which utilizes both the I domain and the Q domain to perform NOMA individually.
- A 2D power allocation method is introduced for JIQ-NOMA that considers both the fairness of users within each user pair and the fairness across different user pairs.
- The performance of the proposed JIQ-NOMA is evaluated and compared with various conventional multi-user transmission schemes through both simulations and experiments.

The rest of this paper is organized as follows: In Section II, we introduce the proposed JIQ-NOMA scheme along with the 2D power allocation method within the context of a general multi-user VLC system. This is followed by the simulation and experimental results in Section III, considering a VLC system with four users. Finally, Section IV concludes the paper.

# II. SYSTEM DESCRIPTION

In this section, we first introduce the user grouping method for the JIQ-NOMA, considering a multi-user VLC system with a general number of users. Next, we explain how the users within a particular group can be supported via the proposed JIQ-NOMA scheme. Finally, we present a 2D power allocation method aimed at enhancing user fairness for the proposed JIQ-NOMA scheme.

# A. User Grouping

In a multi-user VLC system using NOMA, especially with a large number of users, an effective way to support all users is to first organize them into multiple groups. Then, different groups can be supported via OMA techniques, such as OFDMA. Within each group, NOMA is applied by superposing signals intended for different users in the power domain. By denoting the number of groups as K, the overall supported number of users is therefore 4 K. In the following, we introduce a method for grouping these 4 K users according to their channel conditions.

In most LED-based VLC systems, since the DC channel gain between the k-th user and the LED transmitter,  $h_k$ , is usually dominated by the line-of-sight (LOS) components [22], it can be well modeled using

$$h_k = \frac{(m+1)\rho A}{2\pi d_k^2} \cos^m(\psi_k) T(\phi_k) g(\phi_k) \cos(\phi_k), \quad (1)$$

where  $m=-\ln 2/\ln(\cos(\Psi))$  is the Lambertian order of the LED transmitter, with  $\Psi$  being the semi-angle of the LED;  $\rho$  is the responsivity of the photo-diodes (PD) and A is the active area of the PD;  $d_k$  is the distance between the LED and the PD of the k-th user;  $\psi_k$  is the emission angle of the light and  $\phi_k$  is the incident angle of the light;  $T(\phi_k)$  is the transmission coefficient of the optical filter;  $g(\phi_k)=\frac{r^2}{\sin^2\Phi}$  is the gain of the optical lens, with r and  $\Phi$  being the refractive index and the field-of-view (FOV) of the optical lens, respectively. In a multi-user VLC system, the user's position not only affects the transmission distance but also the emission angle and the incident angle of the light. Therefore, the value of  $h_k$  can vary significantly among different users.

To group all 4 K users, they are first arranged in a descending order based on their channel gains obtained using (1), as follows:

$$h_1 \ge \dots \ge h_k \ge \dots \ge h_{4K}. \tag{2}$$

Then, the  $4\,K$  users are divided into four user clusters:  $C_1$ ,  $C_2$ ,  $C_3$ , and  $C_4$ . In these user clusters,  $C_1$  includes the users with relatively high channel gains, which are from User 1 to User K. Following a descending order,  $C_2$  includes users from K+1 to  $2\,K$ ,  $C_3$  includes users from 2K+1 to  $3\,K$ , and  $C_4$  includes users from 3K+1 to  $4\,K$ .

Next, by selecting one user from each user cluster, a group of four users can be formed for JIQ-NOMA implementation. This group is obtained as  $U^i_{\rm group} = [C_1(i), C_2(i), C_3(i), C_4(i)]$  where C(i) represents the ith user in the corresponding user cluster. In JIQ-NOMA, since NOMA is implemented individually in the I and Q domains, two users within a group should form one pair and each group therefore contains two pairs. Similar to conventional NOMA schemes, each user pair consists of a user located relatively far away from the LED, referred to as the far user, and a user located relatively near the LED, referred to as the near user. The first user pair can be formed as  $U^i_{\rm pair,\,Q} = [C_1(i), C_3(i)]$  which is for NOMA implementation in the Q domain. Similarly, the second user pair can be formed as  $U^i_{\rm pair,\,Q} = [C_2(i), C_4(i)]$  which is for NOMA implementation in the I domain. For the case that the number of users does not equal 4K, there will

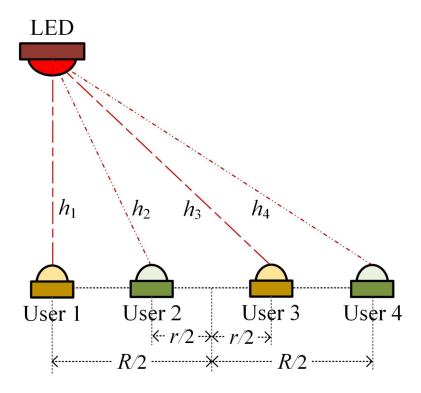


Fig. 1. Illustration of a four-user VLC system.

be one user left unpaired which can be served independently in the I or Q domain. Therefore, the proposed JIQ-NOMA scheme is generally applicable to an arbitrary number of users.

Fig. 1 shows a multi-user VLC system with four users as an example. In this specific example, the locations of User 1 and User 4, as well as User 2 and User 3, are centrosymmetric. We assume that User 1, with the highest channel gain, and User 4, with the lowest channel gain, are at a distance of R from each other. Consequently, the distance from the center to both User 1 and User 4 is R/2. Similarly, we assume that User 2 and User 3 are at a distance of r from each other, and the distance from the center to both User 2 and User 3 is r/2. Using the user grouping method described above, User 1 is paired with User 3, named user pair Q. Their intended signals are superimposed via SPC and transmitted in the Q domain. Similarly, User 2 and User 4 are paired, named user pair I, and their intended signals are superimposed via SPC and transmitted in the I domain.

Although we assume that there are only two users paired together to perform power-domain SPC in the I domain or the Q domain in this current work, it is actually feasible to multiplex more than two users via SPC in the I or Q domain. Hence, the proposed JIQ-NOMA scheme can be generally extended to more than 4 users per group.

# B. Principle of JIQ-NOMA

We now explain the details of the proposed JIQ-NOMA with its schematic diagram shown in Fig. 2. In the JIQ-NOMA transmitter, as illustrated in Fig. 2(a),  $b_{\rm I,n}$  and  $b_{\rm I,f}$  denote the input bit streams to be transmitted to the near user and far user in the user pair I. Similarly,  $b_{\rm Q,n}$  and  $b_{\rm Q,f}$  are the input bit streams to be transmitted to the near user and far user in the user pair Q. Initially, these binary data streams are mapped into PAM constellation symbols to obtain  $x_{\rm I,n}$ ,  $x_{\rm I,f}$ ,  $x_{\rm Q,n}$ ,  $x_{\rm Q,f}$ . Next, the symbols generated for user pair I,  $x_{\rm I,n}$  and  $x_{\rm I,f}$ , remain unchanged. Meanwhile, the symbols intended for user pair Q,  $x_{\rm Q,n}$  and  $x_{\rm Q,f}$ , are rotated by an angle of  $\pi/2$  in the complex constellation space. Subsequently, these symbols are assigned with different power levels and superimposed for transmission. The resulting transmitted symbol is therefore given by

$$x = \sqrt{P_{\rm I,n}} x_{\rm I,n} + \sqrt{P_{\rm I,f}} x_{\rm I,f} + j \left( \sqrt{P_{\rm Q,n}} x_{\rm Q,n} + \sqrt{P_{\rm Q,f}} x_{\rm Q,f} \right),$$
(3)

where  $j=\sqrt{-1}$  represents the imaginary unit,  $P_{\rm I,n}$ ,  $P_{\rm I,f}$ ,  $P_{\rm Q,n}$ , and  $P_{\rm Q,f}$  are the allocated electrical power levels for the signal components intended for different users. As shown in (3),  $x_{\rm I,n}$ ,  $x_{\rm I,f}$ ,  $x_{\rm Q,n}$ ,  $x_{\rm Q,f}$  are now mapped into a complex constellation symbol, which is similar to a conventional quadrature amplitude modulation (QAM) symbol. To transmit these complex constellation symbols, we consider orthogonal frequency division multiplexing (OFDM) modulation, with x transmitted on a single OFDM subcarrier. Similar to typical optical OFDM modulation, the constellation symbols carried on different OFDM subcarriers are constrained to have Hermitian symmetry before undergoing the inverse fast Fourier transform (IFFT) and parallel-to-serial (P/S) conversion. Finally, the resulting time domain JIQ-NOMA signal, s, is used to directly drive the LED for optical signal generation.

In the JIQ-NOMA receiver (Rx), as shown in Fig. 2(b), the received signals from different users,  $y_{I,n}$ ,  $y_{I,f}$ ,  $y_{Q,n}$ , and  $y_{Q,f}$ , first undergo serial-to-parallel (S/P) conversion. Following this, they are transformed into the frequency domain through fast Fourier transform (FFT) so that frequency-domain equalization (FDE) can be performed. Subsequently, the signals transmitted for the user pair Q and the user pair I are obtained by separating the equalized complex symbols in the I domain and the Q domain. Next, for each user pair, similar to the conventional NOMA scheme, the bit stream for the far user can be directly recovered through PAM demapping, while the bit stream for the near user can be obtained through SIC and PAM demapping.

The implementation of SIC-aided detection for JIQ-NOMA with 4 users is illustrated in Fig. 3, where all users are assumed to adopt the 2-PAM constellation. As we can see, the I and Q parts of the received quasi 16-QAM constellation are first separated at the user side, where User 1 and User 3 in user pair Q extract the Q part while User 2 and User 4 in user pair I extract the I part. Specifically, User 3 directly decodes the extracted signal in the Q domain via 2-PAM demapping by treating the 2-PAM signal of User 1 as an interfering signal, while User 1 first decodes the signal for User 3 and then subtracts it from the extracted signal before decoding. Similarly, User 4 directly decodes the extracted signal in the I domain via 2-PAM demapping by treating the 2-PAM signal of User 2 as an interfering signal, while User 2 first decodes the signal for User 4 and then subtracts it from the extracted signal before decoding.

#### C. 2D Power Allocation

As mentioned, in JIQ-NOMA, the allocation of power to different users must account for both the fairness within each user pair and the fairness across different user pairs. To address this issue, we introduce a novel 2D power allocation method in this section. Specifically, we consider both an I/Q power allocation ratio to ensure fairness within each user pair, and a JIQ power allocation ratio to balance the performance differences between two user pairs.

First, similar to conventional NOMA, to balance the performance difference between the far user and the near user within each user pair, their intended signals are allocated with different power levels. This process is referred to as the I/Q

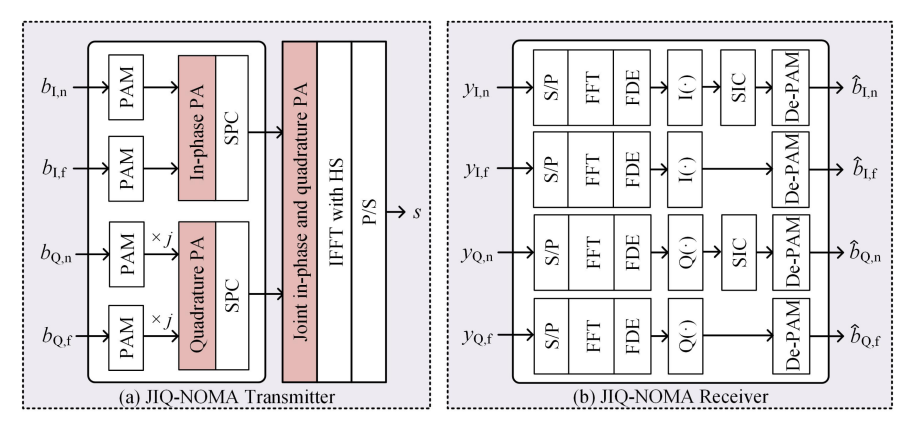


Fig. 2. Schematic diagram of a four-user VLC system applying the proposed JIQ-NOMA scheme (a) JIQ-NOMA transmitter and (b) JIQ-NOMA receiver. PA: Power allocation.

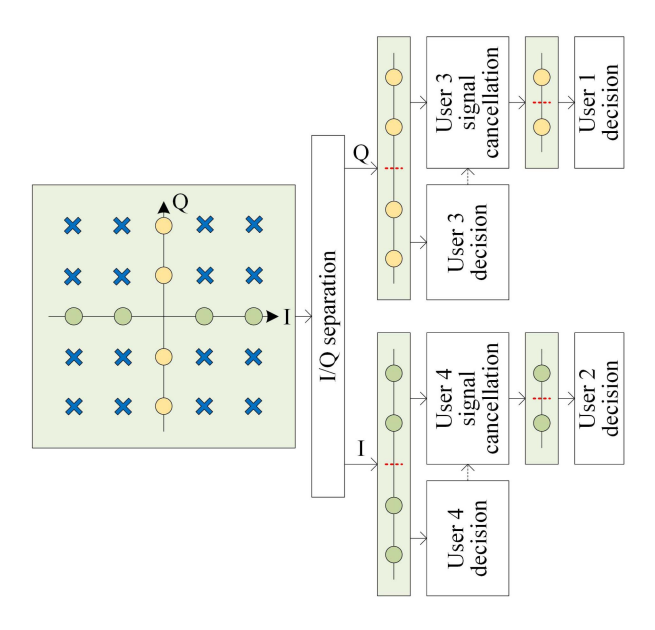


Fig. 3. Illustration of SIC-aided detection for JIQ-NOMA with 4 users.

power allocation. The I/Q power allocation ratios,  $\alpha_{\rm I}$  and  $\alpha_{\rm Q}$  are given by

$$\begin{cases} \alpha_{\rm I} = \frac{P_{\rm Ln}}{P_{\rm l,f}} \\ \alpha_{\rm Q} = \frac{P_{\rm Q,n}}{P_{\rm O,f}} \end{cases}$$
 (4)

Within each user pair, since the far user with a smaller channel gain needs to be allocated more power than the near user with a higher channel gain, we have  $0<\alpha_I<1$  and  $0<\alpha_Q<1$ .

To further balance performance across two different user pairs, a power ratio between signals transmitted via the I channel and the Q channel is also be considered. This power allocation ratio is referred to as the JIQ power allocation ratio and is given by

$$\beta = \frac{P_{\rm Q}}{P_{\rm I}},\tag{5}$$

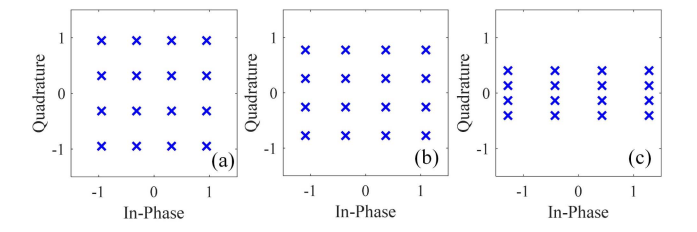


Fig. 4. Constellation diagram of JIQ power ratio (a)  $\beta=1$  , (b)  $\beta=0.5$  , and (c)  $\beta=0.1$ 

where

$$\begin{cases}
P_{\rm I} = P_{\rm I,n} + P_{\rm I,f} = (1 + \alpha_{\rm I}) P_{\rm I,f} \\
P_{\rm Q} = P_{\rm Q,n} + P_{\rm Q,f} = (1 + \alpha_{\rm Q}) P_{\rm Q,f}
\end{cases}$$
(6)

are the overall allocated electrical power levels to the user pair I and the user pair Q, respectively. Without loss of generality, we assume that user pair I has a smaller overall channel gain than user pair Q and thus it is reasonable to allocate more power to user pair I. As a result, we have  $0 < \beta < 1$ .

To illustrate the relationship between the shape of the constellation and the JIQ power allocation ratio,  $\beta$ , Fig. 4 shows the constellation diagrams for various values of  $\beta$ . It can be seen that different values of  $\beta$  impact the distribution of constellation points. In Fig. 4(a), where  $\beta=1$ , signals in the I domain and Q domain have equal power, resulting in a square-shaped constellation distribution. In contrast, as shown in Fig. 4(c), when  $\beta=0.1$ , the signal in the Q domain has a lower power level compared to the signal in the I domain. This results in a smaller overall amplitude in the Q domain, shaping the constellation distribution into a rectangle. As  $\beta$  decreases, the composite signal's constellation remains a rectangular shape with an increasing difference between its length and width.

In the case, when the overall allocated electrical power is denoted as  $P_{\text{tot}} = P_{\text{I}} + P_{\text{Q}}$ ,  $P_{\text{I}}$  and  $P_{\text{Q}}$  can be also given by

$$\begin{cases}
P_{\rm I} = \frac{P_{\rm tot}}{1+\beta} \\
P_{\rm Q} = \frac{\beta P_{\rm tot}}{1+\beta}
\end{cases}$$
(7)

TABLE I SIMULATION PARAMETERS

Parameter	Value
Vertical separation	2.15 m
Semi-angle at half power of LED	$70^{\circ}$
Gain of optical filter	0.9
Refractive index of optical lens	1.5
Half-angle FOV of optical lens	$70^{\circ}$
Responsivity of PD	0.53  A/W
Active area of PD	$1 \text{ cm}^2$
Signal bandwidth	10 MHz
Noise power spectral density	$10^{-22} \text{ A}^2/\text{Hz}$
Modulation scheme	2-PAM

Thus, combining (6) and (7), the allocated power levels of the far user and the near user within the user pair I can be expressed as a function of  $P_{\text{tot}}$ ,  $\alpha_{\text{I}}$ ,  $\beta$  using

$$\begin{cases} P_{\rm I,f} = \frac{P_{\rm I}}{1+\alpha_{\rm I}} = \frac{P_{\rm tot}}{(1+\alpha_{\rm I})(1+\beta)}, \\ P_{\rm I,n} = \frac{\alpha_{\rm I}P_{\rm I}}{1+\alpha_{\rm I}} = \frac{\alpha_{\rm I}P_{\rm tot}}{(1+\alpha_{\rm I})(1+\beta)}, \end{cases}$$
(8)

similarly, the allocated power levels of the far user and the near user of the user pair Q can be given by

$$\begin{cases} P_{\mathrm{Q,f}} = \frac{P_{\mathrm{Q}}}{1+\alpha_{\mathrm{Q}}} = \frac{\beta P_{\mathrm{tot}}}{(1+\alpha_{\mathrm{Q}})(1+\beta)} \\ P_{\mathrm{Q,n}} = \frac{\alpha_{\mathrm{Q}} P_{\mathrm{Q}}}{1+\alpha_{\mathrm{Q}}} = \frac{\beta \alpha_{\mathrm{Q}} P_{\mathrm{tot}}}{(1+\alpha_{\mathrm{Q}})(1+\beta)} \end{cases}$$
(9)

Besides 2D power allocation, a hybrid JIQ-NOMA/OFDMA scheme can also be designed to satisfy the users' bandwidth requirements via subcarrier allocation. Moreover, a generalized multiple access (GMA) scheme based on JIQ-NOMA can be further developed to jointly allocate subcarrier (i.e., bandwidth) and power for different users in the I or Q domain individually. For more details about the principle of GMA, please refer to our previous work [23].

# III. RESULTS AND DISCUSSIONS

Next, we show how the optimal values of  $\alpha_I$ ,  $\alpha_Q$ ,  $\beta$  can be obtained, referred to as the 2D power allocation method. Furthermore, we evaluate the performance of the proposed JIQ-NOMA scheme and compare it with conventional NOMA and OMA schemes via both simulations and experiments.

#### A. Simulation Results

The VLC scenario illustrated in Fig. 1 is considered in our simulation. In this setup, the LED is positioned above the users with a vertical distance of 2.15 m. The horizontal separation between User 1 and User 4, R, is fixed at 2 m. As mentioned, User 1 and User 3 form the user pair Q, while User 2 and User 4 form the user pair I. In this work, we also defined  $\zeta = r/R$  as a parameter to represent the channel difference between user pair I and user pair Q. In particular, we consider three different values of  $\zeta$ : 0.1, 0.4, and 0.7.  $\zeta = 0.1$  indicates a significant difference in channel gain between the two user pairs.  $\zeta = 0.4$  denotes a moderate difference, and  $\zeta = 0.7$  means the channel gain difference is relatively minor. Other simulation parameters are listed in Table I. With these simulation parameters, the channel gain in our simulation is on the order of  $10^{-6}$ , implying that

the transmitted signal-to-noise ratio (SNR), defined as the ratio between the power of the transmitted signal and the power of the noise at the receiver, should be above 120 dB.

To ensure user fairness within each pair, we first determine the optimal I/Q power allocation ratio,  $\alpha$ , individually for both user pair Q and user pair I. In Fig. 5, the simulated bit error rate (BER) is plotted as a function of  $\alpha$  when the transmitted SNR is 130 dB. The results show that within each user pair, an increase in  $\alpha$  leads to a gradual increase in the BER of the far user. However, for the near user, the BER first decreases and then increases. This is because an increase in  $\alpha$  means less power is assigned to the far user, thereby increasing its BER. For the near user, an increase in  $\alpha$  initially decreases the BER, but when  $\alpha$  becomes too high, the reduced power assigned to the far users causes a significant amount of detection errors which can propagate into the data decoding process of the near user, eventually increasing the BER. For both user pair Q and user pair I, the average BER is minimized when the BERs of the near and far users are close. This also explains the importance of considering user fairness in the transmission. The results show that for  $\zeta$  values of 0.1, 0.4, and 0.7, the optimal  $\alpha$  values for user pair Q are 0.2, 0.15, and 0.1, respectively. For user pair I, the corresponding optimal  $\alpha$  values are 0.15, 0.15, and 0.1. In these three scenarios, as  $\zeta$ increases, the differences between user pairs decrease, and the average BER of user pair Q and user pair I become increasingly similar. However, there still remain differences between the two user pairs after I/Q power allocation. Therefore, the JIQ power allocation is performed at the next step.

To obtain the optimal value of the JIQ power allocation ratio,  $\beta$ , we first fix  $\alpha$  at its optimal values which are obtained in the above step. Then, Fig. 6 shows the simulated BER versus  $\beta$  when the considered  $\zeta$  values are 0.1, 0.4, and 0.7. We can see that increasing  $\beta$  reduces the BER of the Q channel while increasing the BER of the I channel. This is because a higher value of  $\beta$ means more power is allocated to the signals intended for the users in the pair Q, and less power is allocated to the users in the pair I. Also, it can be seen that the average BER first increases and then decreases and the optical value of  $\beta$  can be obtained when the user pair Q and the user pair I have the same BER. Moreover, the results show that the optimal value of  $\beta$  changes for different values of  $\zeta$ . This is because a higher value of  $\zeta$ means that channel differences between different user pairs are reduced, and therefore the optimal  $\beta$  value is closer to one. In the examples shown in Fig. 6, the optimal  $\beta$  is 0.4, 0.6, and 0.7 when  $\zeta$  is 0.1, 0.4, and 0.7, respectively. Then, after obtaining the optimal I/Q power allocation ratio,  $\alpha$ , and JIQ power allocation ratio,  $\beta$ , the optimal JIQ-NOMA scheme is determined.

Next, to better illustrate how JIQ power allocation can affect the shape of the generated constellation and, therefore, lead to similar performance between different users, Figs. 7(a)–(d) show the simulated received constellation of four users when the transmitted SNR is 130 dB and  $\zeta=0.6$ . In this example, using the 2D power allocation method, the obtained optimal I/Q power allocation ratios are  $\alpha_{\rm I}=0.1$  and  $\alpha_{\rm Q}=0.15$ , and the optimal JIQ power allocation ratio is  $\beta=0.6$ . With the 2D power allocation, as expected, it can be seen that the shape of the constellation is rectangular. Additionally, it is observed

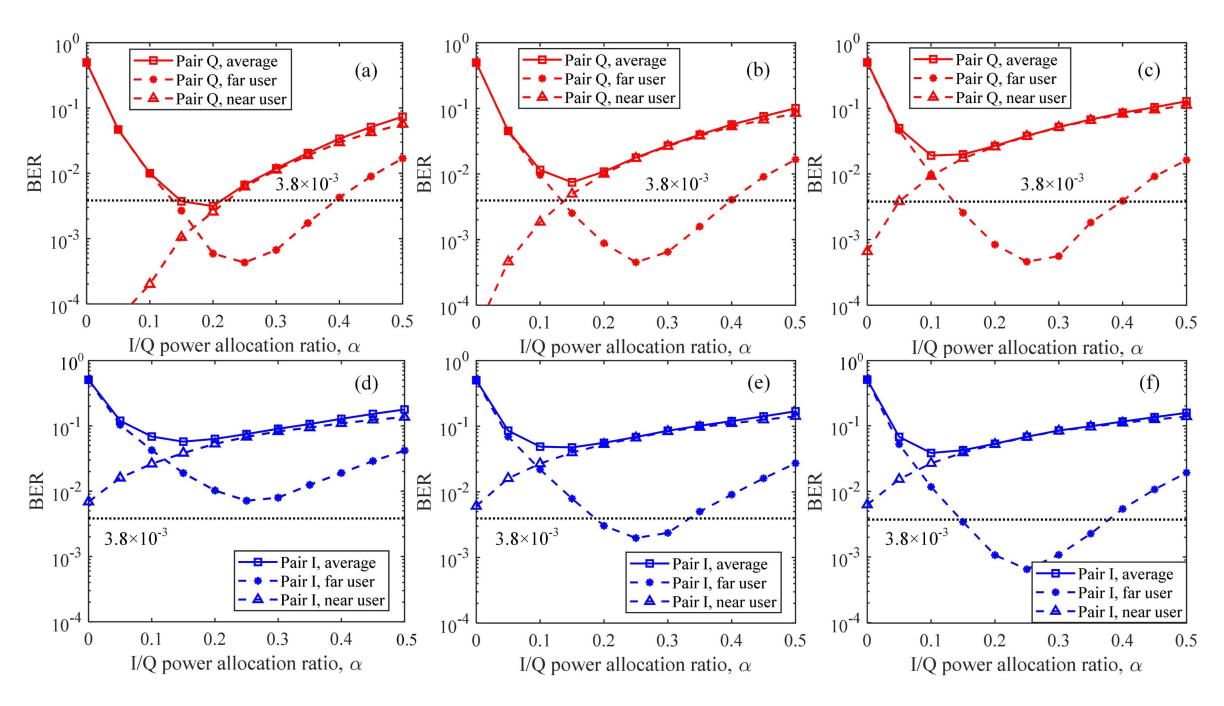


Fig. 5. Simulation BER vs. I/Q power allocation ratio  $\alpha$  for (a) Pair Q,  $\zeta=0.1$ , (b) Pair Q,  $\zeta=0.4$ , (c) Pair Q,  $\zeta=0.7$ , (d) Pair I,  $\zeta=0.1$ , (e) Pair I,  $\zeta=0.4$ , and (f) Pair I,  $\zeta=0.7$ .

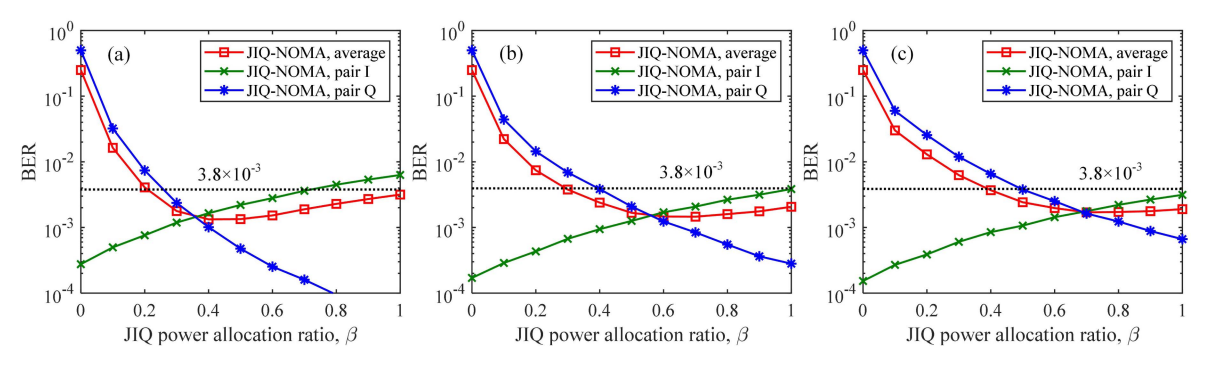


Fig. 6. Simulation BER vs. JIQ power allocation ratio  $\beta$  for (a)  $\zeta = 0.1$ , (b)  $\zeta = 0.4$ , and (c)  $\zeta = 0.7$ .

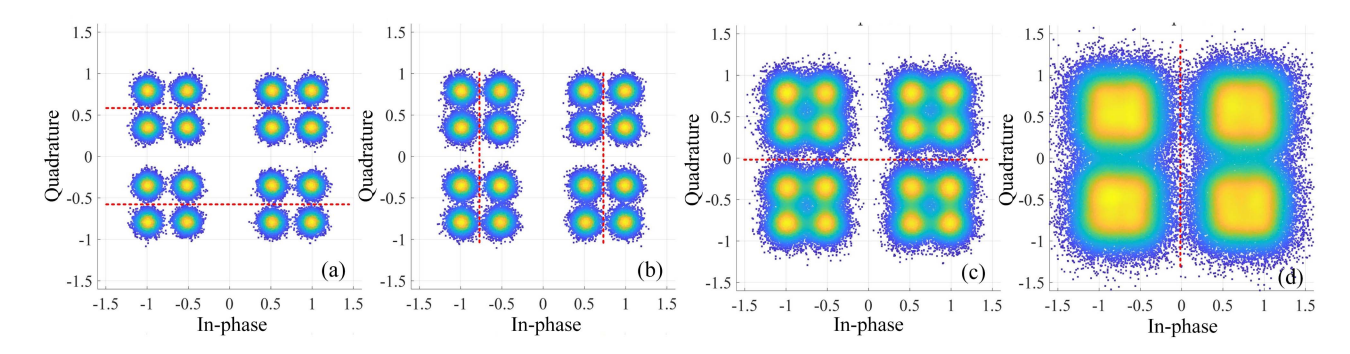


Fig. 7. The simulated JIQ-NOMA constellations of (a) User 1, (b) User 2, (c) User 3, and (d) User 4, when  $\alpha_{\rm I}=0.1, \alpha_{\rm Q}=0.15, \beta=0.6$ .

that, due to the differences in channel conditions between these users, their noise components in the received constellations vary significantly. To explain how the noise can affect the detection performance of four different users, the maximum likelihood (ML) hard decision boundaries highlighted in red are also shown in the Euclidean space. However, note that for User 1 and User 2, the decision boundaries are only estimations. This is because after performing SIC, the distribution of their constellations will

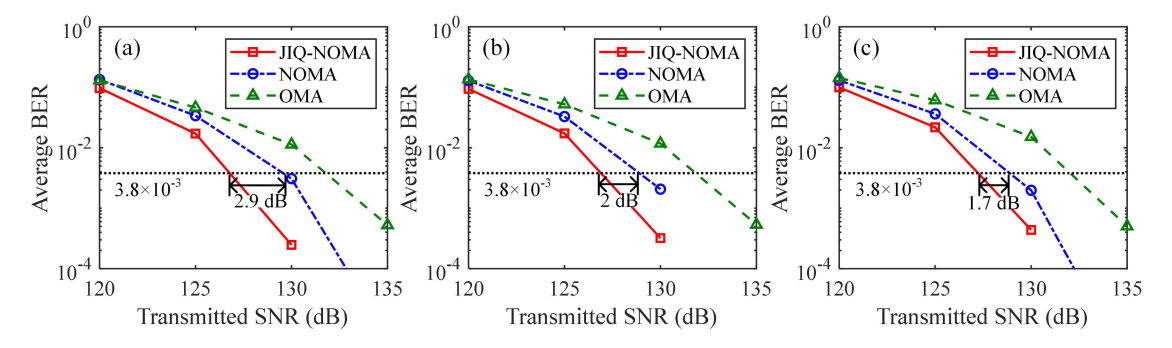


Fig. 8. Simulation average BER vs. transmitted SNR for (a)  $\zeta = 0.1$ , (b)  $\zeta = 0.4$ , and (c)  $\zeta = 0.7$ .

be affected due to the error propagation effect. However, since the error propagation effect is relatively low in this example, we use these boundaries to intuitively explain why these users have similar performance despite their significantly different noise levels. First, when comparing the performance of users within each user pair, i.e., User 1 and User 3, it can be seen that due to the consideration of the I/Q power allocation, the two users exhibit very similar performance, even though the noise level for the far user is much higher. Then, we compare the performance between two different user pairs. Due to the consideration of the JIQ power allocation ratio, the symbols have more power in the I domain than in the Q domain. This is particularly obvious in the case of User 4. It can be seen from Fig. 7(d) that, although the constellations highly overlap in the Q domain, this overlap is significantly lower in the I domain. Therefore, the performance of User 4 in pair I is still very similar to the two users in pair Q. Overall, although the four users have very different channel conditions, due to the use of power allocation, they all exhibit very similar performance.

Then, we compare the performance of three different multiuser transmission schemes: OMA, NOMA, and JIQ-NOMA via simulation. For the JIQ-NOMA scheme, we employ the described method to determine the optimal I/Q power allocation ratios,  $\alpha_{\rm I}$  and  $\alpha_{\rm Q}$ , and the JIQ power allocation ratio,  $\beta$ . For comparison purposes, in the conventional four-user NOMA scheme, 4-QAM is employed for each user. Additionally, the signals intended for User 1 and User 3 are superimposed in the power domain, while the signals intended for User 2 and User 4 are superimposed in the power domain. Also, unlike the proposed JIQ-NOMA, the two superimposed signals are multiplexed via OFDMA. To ensure a fair comparison, we also consider the optimal power allocation ratio for each user pair in the conventional NOMA scheme. Considering the 7% forward error correction (FEC) limit of BER =  $3.8 \times 10^{-3}$ , Fig. 8 shows that the proposed JIQ-NOMA scheme requires a much lower transmitted SNR compared to the conventional NOMA and OMA schemes. In particular, compared with the conventional NOMA scheme, the required transmitted SNR of the proposed JIQ-NOMA scheme to achieve the FEC limit is reduced by 2.9 dB, 2 dB, and 1.7 dB when  $\zeta = 0.1$ , 0.4, and 0.7, respectively. This means that the advantage of using the proposed JIQ-NOMA scheme becomes more obvious when there is a significant difference in channel gains among different user pairs.

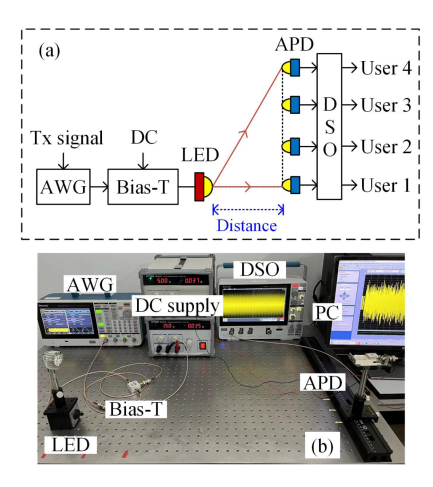


Fig. 9. (a) Experimental setup of a four-user VLC system and (b) the photo of the experimental testbed.

# TABLE II EXPERIMENTAL PARAMETERS

Parameter	Value
AWG sampling rate	20 MSa/s
DC voltage	1.5 V
DC current	35 mA
Tx peak-to-peak voltage	$1\sim 2.5 \text{ V}$
Rx active area	1.5 mm
APD voltage	5 V
DSO sampling rate	100 MSa/s
Modulation scheme	2-PAM
IFFT/FFT size	256
Number of data subcarriers	92
Transmission distance	$70 \sim 100 \text{ cm}$

# B. Experimental Results

We also conducted experiment measurements to investigate the performance of the proposed JIQ-NOMA scheme in a practical multi-user VLC system. The experimental setup of a four-user VLC system is shown in Fig. 9(a), and a photo of the experimental testbed is presented in Fig. 9(b). The key experimental parameters are listed in Table II. At the transmitter side, JIQ-NOMA signals were first generated offline using MATLAB and then sent to an arbitrary waveform generator (AWG, Tektronix AFG31102) with a transmission sampling rate of 20 MSa/s. Subsequently, the signal output from the AWG was superimposed onto a 35 mA DC current via a bias-tee (bias-T,

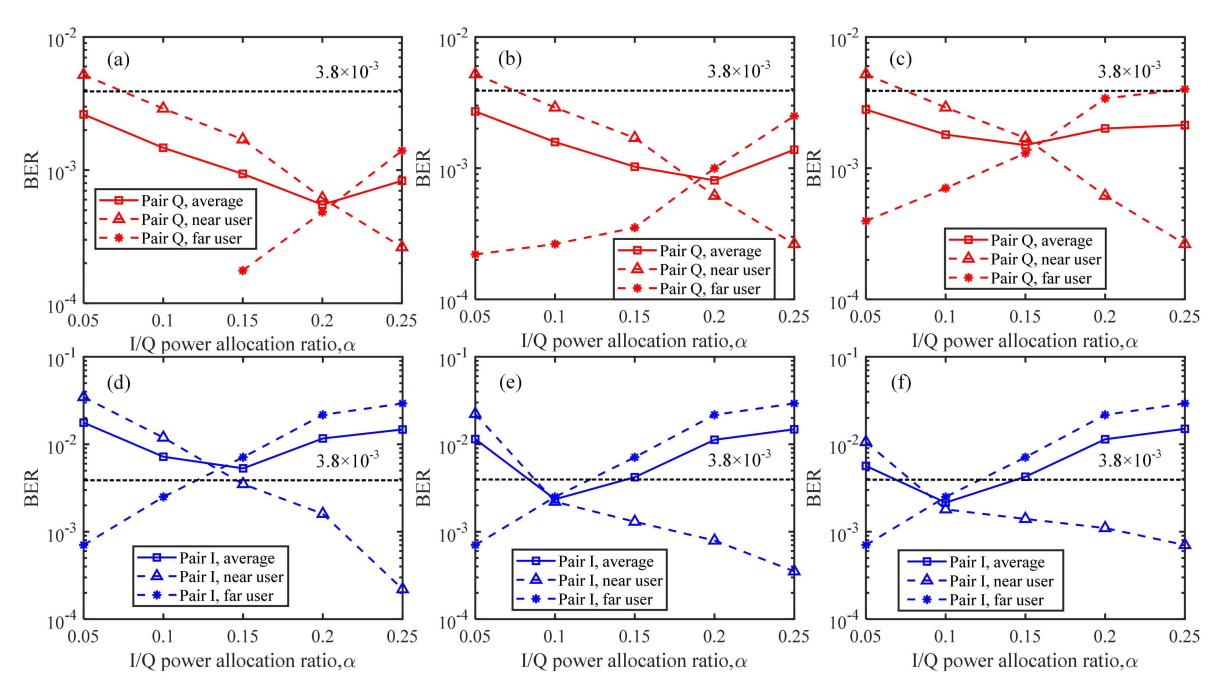


Fig. 10. Experimental BER vs. I/Q power allocation ratio  $\alpha$  for (a) Pair Q,  $\zeta=0.1$ , (b) Pair Q,  $\zeta=0.4$ , (c) Pair Q,  $\zeta=0.7$ , (d) Pair I,  $\zeta=0.1$ , (e) Pair I,  $\zeta=0.4$ , and (f) Pair I,  $\zeta=0.7$ .

MiniCircuits, ZFBT-6GW+) to drive a commercially available LED. At the receiver side, an avalanche photo-diode (APD, Hamamatsu C12702-12) was used to detect the optical signal. The received signal from the APD was then captured by a digital storage oscilloscope (DSO, LeCroy WaveSurfer 432) with a sampling rate of 100 MSa/s which was further processed offline using MATLAB to recover the transmitted data. Also, based on the user location arrangement illustrated in Fig. 9(a), the APD was placed at four different positions for signal capturing so that the received signals of four different users were obtained. In this setup, both the LED and the APD were placed on the same height above the optical bench. The distance between the LED and the line where the APD moved on was 80 cm and the distance between User 1 and User 4, *R*, was considered as 20 cm.

Similar to the simulations, the 2D power allocation process involves first obtaining the optimal I/Q power allocation ratios,  $\alpha$ , for each user pair. Fig. 10 shows the experimental BER versus  $\alpha$ for both user pair Q and user pair I with different  $\zeta$  values. Based on the previously presented simulation results, it can be seen that the optimal  $\alpha$  is around 0.2. In the experimental measurements, instead of assessing the system's performance by considering all possible values of  $\alpha$ , we only considered  $\alpha$  that are close to their optimal value obtained through simulations. Within the considered range of  $\alpha$ , as  $\alpha$  increases, the BER of the near user gradually decreases, while the BER of the far user increases. Similar to simulation results, for both user pair Q and user pair I, the minimum average BERs are obtained when the BERs of the near user and the far user are similar. The measurement results show that, for  $\zeta = 0.1, 0.4$ , and 0.7, the optimal  $\alpha$  values for user pair Q are 0.2, 0.2, and 0.15, respectively. For user pair I, the optimal  $\alpha$  values are 0.15, 0.1, and 0.1, respectively. Consistent with our findings in the simulations, as  $\zeta$  increases, since the channel difference between the two users within each user pair becomes large, the optimal  $\alpha$  becomes smaller.

After obtaining the optimal I/Q power allocation ratio  $\alpha$  for each user pair, we further determine the optimal JIQ power allocation ratio  $\beta$ . Figs. 11(a)–(c) show the measured BER versus the JIQ power allocation ratio  $\beta$  for  $\zeta$  values of 0.1, 0.4, and 0.7, respectively. As expected, the BER of user pair I gradually decreases with increasing  $\beta$ , while the BER of user pair Q gradually increases. The optimal  $\beta$  values associated with the minimum average BERs are 0.4, 0.7, and 0.7 for  $\zeta$  = 0.1, 0.4, and 0.7, respectively. This observation aligns with our simulation results, indicating that as  $\zeta$  increases, the differences between user pairs decrease, leading to higher optimal values of  $\beta$ .

Next, we show the received constellations of different users obtained in our experiment, and the results are presented in Fig. 12. Consistent with the simulation results shown in Fig. 7, the shape of the constellation is rectangular, indicating the higher power allocation for I pair users compared to Q pair users. Despite the varying channel conditions among these users leading to different noise levels, the transmitted data for them can be decoded with very similar performance. For instance, even though User 4 experiences a significantly high noise level, as its transmitted data is carried in the Q domain, it can still be decoded with a BER lower than the FEC limit.

After obtaining the optimal values of  $\alpha$  and  $\beta$ , we measured the performance of the proposed JIQ-NOMA scheme and compared it with conventional NOMA and OMA schemes. In Fig. 13(a)–(c), we present the measured average BER with different peak-to-peak voltage (Vpp) of the AWG output signal. Various values of Vpp were considered so that the power of the transmitted signal could be adjusted, enabling the investigation into the influences of various received SNRs on the system

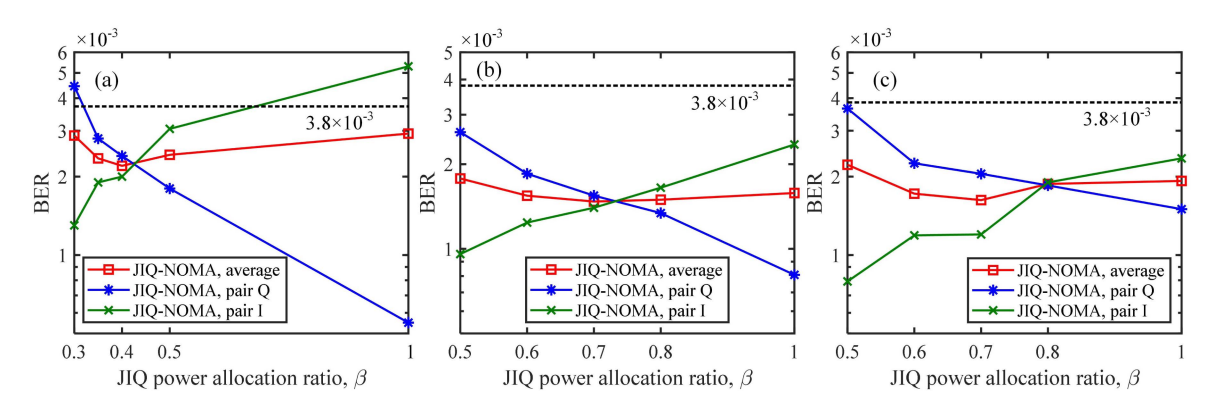


Fig. 11. Experimental BER vs. JIQ power allocation ratio  $\beta$  for (a)  $\zeta = 0.1$ , (b)  $\zeta = 0.4$ , and (c)  $\zeta = 0.7$ .

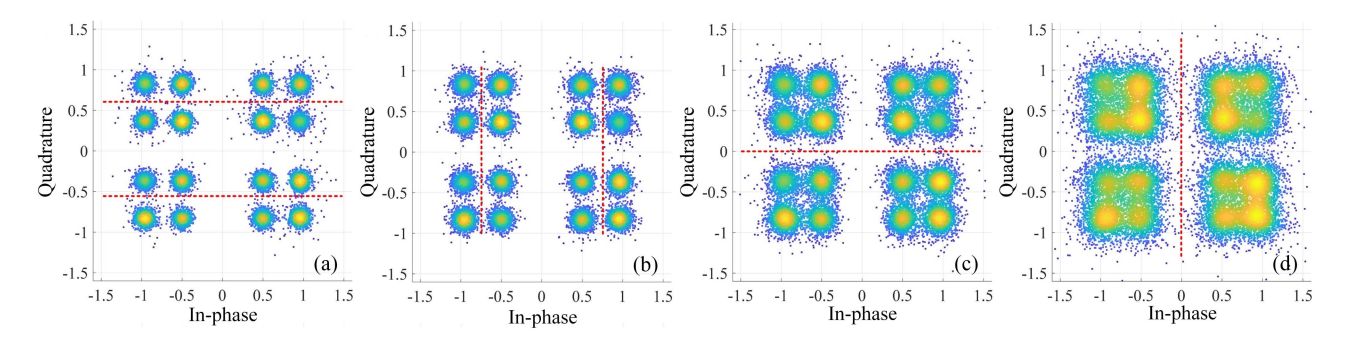


Fig. 12. The received JIQ-NOMA constellations obtained in experimental measurements of (a) User 1, (b) User 2, (c) User 3, and (d) User 4, when  $\alpha_{\rm I}=0.1$ ,  $\alpha_{\rm Q}=0.15$ ,  $\beta=0.6$ .

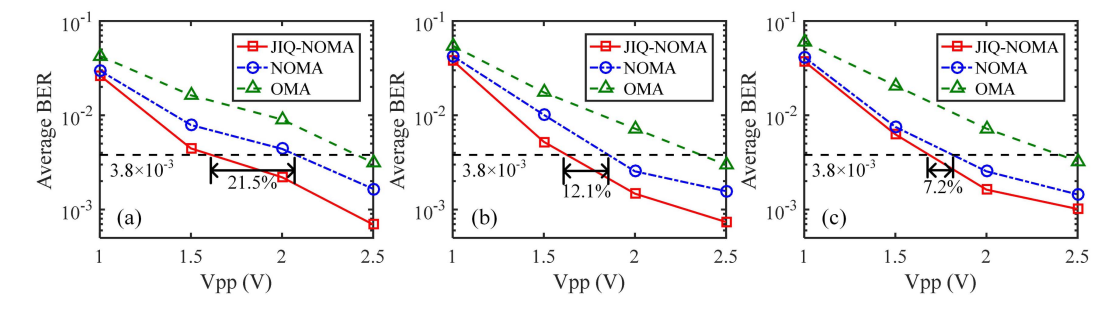


Fig. 13. Experimental average BER vs. Vpp for (a)  $\zeta = 0.1$ , (b)  $\zeta = 0.4$ , and (c)  $\zeta = 0.7$ .

performance. As shown in Fig. 13(a)–(c), it can be seen that average BER reduces with an increase in Vpp. Moreover, to meet the FEC limit, the differences in the required Vpp between NOMA and JIQ-NOMA are 21.5%, 12.1%, and 7.2% for  $\zeta=0.1,0.4$ , and 0.7, respectively. Also, it is noticeable that the average BER of JIQ-NOMA and NOMA schemes becomes closer as  $\zeta$  increases. This is because when  $\zeta$  increases, the distance between two users in one user pair increases, while the difference between two user pairs decreases. This means that the optimal  $\beta$  is increased, and optimal  $\alpha$  is decreased in JIQ-NOMA, making it more similar to the conventional NOMA scheme. However, the proposed JIQ-NOMA scheme consistently achieves better performance than the conventional NOMA scheme.

Another way to vary the received signal strength of different users is by changing the transmission distance. Therefore, we measured the average BER versus transmission distance for three different multiple access schemes, and the results are shown in Fig. 14. In this experiment, optimal values of  $\alpha$  and  $\beta$  were determined at each considered transmission distance, and three values of  $\zeta$  were also considered. First, it can be seen that both NOMA and JIQ-NOMA can significantly outperform OMA. Furthermore, when  $\zeta$  is 0.1, our proposed JIQ-NOMA can result in a maximum transmission distance of 91 cm when the measured BER is below the 7% FEC limit. Comparison with the conventional NOMA scheme, the maximum transmission distance is increased by 16.7%. When  $\zeta$  is 0.4, the JIQ-NOMA scheme can achieve a maximum transmission distance of 96.5 cm, with an increase of 12.2% compared to the conventional NOMA scheme. When  $\zeta$  is 0.7, the increase becomes 7.9%.

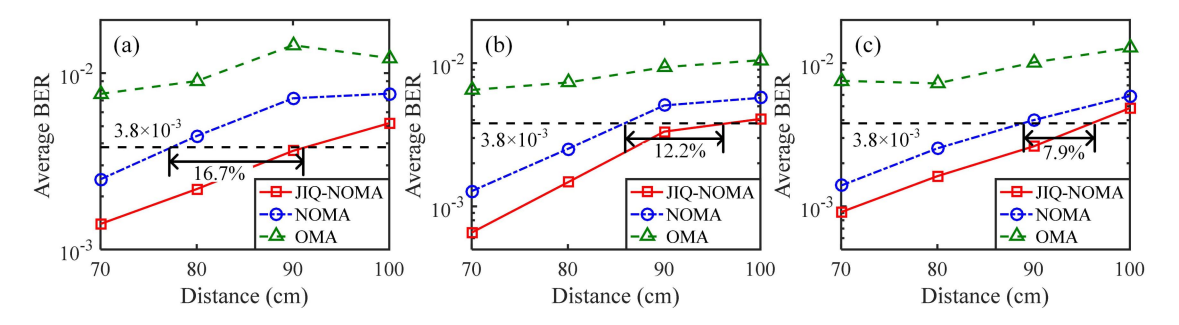


Fig. 14. Experimental average BER vs. distance for (a)  $\zeta=0.1$ , (b)  $\zeta=0.4$ , and (c)  $\zeta=0.7$ .

# IV. CONCLUSION

In this paper, we propose and experimentally demonstrate a novel JIQ-NOMA scheme for multi-user VLC systems. Different from the conventional NOMA scheme, the proposed JIQ-NOMA utilizes both the I domain and the Q domain to perform NOMA individually. This introduces an additional degree of freedom for power allocation, further enhancing user fairness in multi-user VLC systems. To optimize its performance, we introduce a 2D power allocation method, which considers both the channel differences within each user pair and the channel differences between two user pairs. Simulation and experimental results show that JIQ-NOMA significantly outperforms conventional NOMA and OMA schemes. In particular, our simulation results demonstrate that the proposed JIQ-NOMA requires much lower transmitted SNRs to achieve the same BER level. In practical experiments, this means a significant reduction in the required power of the transmitter and/or an increase in the transmission distance while supporting the same number of users. In our future work, we will consider the application of JIQ-NOMA in multiple-input multiple-output VLC systems and multi-cell VLC systems. Moreover, users' quality-of-service requirements will also be taken into consideration to develop new user grouping strategies for JIQ-NOMA.

# REFERENCES

- P. Yang, Y. Xiao, M. Xiao, and S. Li, "6G wireless communications: Vision and potential techniques," *IEEE Netw.*, vol. 33, no. 4, pp. 70–75, Jul./Aug. 2019.
- [2] N. Chi, Y. Zhou, Y. Wei, and F. Hu, "Visible light communication in 6G: Advances, challenges, and prospects," *IEEE Veh. Technol. Mag.*, vol. 15, no. 4, pp. 93–102, Dec. 2020.
- [3] C. Chen, S. Fu, X. Jian, M. Liu, X. Deng, and Z. Ding, "NOMA for energy-efficient LiFi-enabled bidirectional IoT communication," *IEEE Trans. Commun.*, vol. 69, no. 3, pp. 1693–1706, Mar. 2021.
- [4] L. E. M. Matheus, A. B. Vieira, L. F. M. Vieira, M. A. M. Vieira, and O. Gnawali, "Visible light communication: Concepts, applications and challenges," *IEEE Commun. Surv. Tuts.*, vol. 21, no. 4, pp. 3204–3237, Fourthquarter 2019.
- [5] I. Demirkol, D. Camps-Mur, J. Paradells, M. Combalia, W. Popoola, and H. Haas, "Powering the Internet of Things through light communications," *IEEE Commun. Mag.*, vol. 57, no. 6, pp. 107–113, Jun. 2019.
- [6] Z. Ghassemlooy, S. Arnon, M. Uysal, Z. Xu, and J. Cheng, "Emerging optical wireless communications-advances and challenges," *IEEE J. Sel. Areas Commun.*, vol. 33, no. 9, pp. 1738–1749, Sep. 2015.

- [7] T. Komine and M. Nakagawa, "Fundamental analysis for visible-light communication system using LED lights," *IEEE Trans. Consum. Electron.*, vol. 50, no. 1, pp. 100–107, Feb. 2004.
- [8] T. Cogalan and H. Haas, "Why would 5G need optical wireless communications?," in *Proc. IEEE Ann. Int. Symp. Pers., Indoor Mobile Radio Commun.*, 2017, pp. 1–6.
- [9] S. Rajagopal, R. D. Roberts, and S.-K. Lim, "IEEE 802.15.7 visible light communication: Modulation schemes and dimming support," *IEEE Commun. Mag.*, vol. 50, no. 3, pp. 72–82, Mar. 2012.
- [10] M. Obeed, A. M. Salhab, M.-S. Alouini, and S. A. Zummo, "On optimizing VLC networks for downlink multi-user transmission: A survey," *IEEE Commun. Surv. Tuts.*, vol. 21, no. 3, pp. 2947–2976, Thirdquarter 2019.
- [11] A. M. Abdelhady, O. Amin, A. Chaaban, B. Shihada, and M.-S. Alouini, "Downlink resource allocation for dynamic TDMA-based VLC systems," *IEEE Trans. Wireless Commun.*, vol. 18, no. 1, pp. 108–120, Jan. 2019.
- [12] J.-Y. Sung, C.-H. Yeh, C.-W. Chow, W.-F. Lin, and Y. Liu, "Orthogonal frequency-division multiplexing access (OFDMA) based wireless visible light communication (VLC) system," *Opt. Commun.*, vol. 355, pp. 261–268, Nov. 2015.
- [13] Y. Qiu, S. Chen, H.-H. Chen, and W. Meng, "Visible light communications based on CDMA technology," *IEEE Wireless Commun.*, vol. 25, no. 2, pp. 178–185, Apr. 2018.
- [14] H. Marshoud, V. M. Kapinas, G. K. Karagiannidis, and S. Muhaidat, "Non-orthogonal multiple access for visible light communications," *IEEE Photon. Technol. Lett.*, vol. 28, no. 1, pp. 51–54, Jan. 2016.
- [15] H. Marshoud, P. C. Sofotasios, S. Muhaidat, G. K. Karagiannidis, and B. S. Sharif, "On the performance of visible light communication systems with non-orthogonal multiple access," *IEEE Trans. Wireless Commun.*, vol. 16, no. 10, pp. 6350–6364, Oct. 2017.
- [16] C. Chen, W.-D. Zhong, H. Yang, and P. Du, "On the performance of MIMO-NOMA-based visible light communication systems," *IEEE Pho*ton. Technol. Lett., vol. 30, no. 4, pp. 307–310, Feb. 2018.
- [17] C. Chen, W.-D. Zhong, H. Yang, P. Du, and Y. Yang, "Flexible-rate SIC-free NOMA for downlink VLC based on constellation partitioning coding," IEEE Wireless Commun. Lett., vol. 8, no. 2, pp. 568–571, Apr. 2019.
- [18] J. A. L. Silva et al., "Performance evaluation of a simplified power-domain NOMA for visible light communications," *J. Opt. Soc. Amer. A*, vol. 40, pp. C46–C52, Apr. 2023.
- [19] L. Yin, W. O. Popoola, X. Wu, and H. Haas, "Performance evaluation of non-orthogonal multiple access in visible light communication," *IEEE Trans. Commun.*, vol. 64, no. 12, pp. 5162–5175, Dec. 2016.
- [20] B. Lin, W. Ye, X. Tang, and Z. Ghassemlooy, "Experimental demonstration of bidirectional NOMA-OFDMA visible light communications," *Opt. Exp.*, vol. 25, no. 4, pp. 4348–4355, Feb. 2017.
- [21] C. Chen, Y. Tang, Y. Cai, and M. Liu, "Fairness-aware hybrid NOMA/OFDMA for bandlimited multi-user VLC systems," *Opt. Exp.*, vol. 29, no. 25, pp. 42265–42275, Dec. 2021.
- [22] L. Zeng et al., "High data rate multiple input multiple output (MIMO) optical wireless communications using white LED lighting," *IEEE J. Sel. Areas Commun.*, vol. 27, no. 9, pp. 1654–1662, Dec. 2009.
- [23] Y. Tang, C. Chen, M. Liu, P. Du, and H. Y. Fu, "Rate-splitting-based generalized multiple access for band-limited multi-user VLC," *Photonics*, vol. 10, no. 4, 2023, Art. no. 446.